

TEMPERLEY–LIEB ALGEBRAS AND p -KAZHDAN–LUSZTIG THEORY

CHRIS BOWMAN

ABSTRACT. The past decade has seen categorification upend the field of representation theory through the resolution of the field’s oldest and most famous conjectures. We introduce the main players and ideas in this area, making them more manageable by restricting our attention to the most combinatorially well-understood families.

INTRODUCTION

Real reflection groups are the linchpin for the construction of all Lie theoretic objects: Lie groups, reductive algebraic groups, Kac–Moody Lie algebras, and finite groups of Lie type. Kazhdan–Lusztig’s positivity conjecture states that much of geometric Lie theory should generalise beyond the realm of real reflection groups to arbitrary Coxeter groups. However, this is precisely the point at which the geometric structures dissolve entirely. The central idea of 21st century Lie theory has been to replace geometric constructions with wider reaching categorical analogues. The Hecke categories provide the structural perspective in which the Kazhdan–Lusztig positivity conjecture was recently proven and in which counterexamples to the expected bounds in Lusztig’s conjecture were found.

In this series of lectures we give a concrete and hands-on introduction to the Hecke category. In order to accelerate understanding, we simplify things by considering the case in which “Temperley–Lieb”-style combinatorics governs the Kazhdan–Lusztig-theory. We also discuss how these ideas were used by Williamson and Elias–Williamson to (dis)prove the Lusztig conjecture and Kazhdan–Lusztig positivity conjecture. We also talk a little bit about where the field is now going...in particular the development of a new generational philosophy of Lusztig–Williamson and Libedinsky–Patimo–Plaza which seeks to understand the characters and cohomological structure of Lie theoretic objects in positive characteristic.

1. KAZHDAN–LUSZTIG THEORY

Kazhdan–Lusztig theory is the study of walks in coset graphs for parabolic Coxeter systems. Kazhdan–Lusztig theory controls the representation theory of Lie theoretic objects. This course will focus on the examples in which we can completely understand Kazhdan–Lusztig polynomials and the algebraic objects they control. This means “Catalan” or “Temperley–Lieb” combinatorics and algebras.

1.1. A parabolic Coxeter system. Our favourite group is the symmetric group, with presentation

$$\mathfrak{S}_n = \langle s_i = (i, i + 1), 1 \leq i < n \mid s_i^2 = 1, (s_i s_{i+1})^3 = 1, (s_i s_j)^2 = 1 \text{ for } |i - j| > 1 \rangle$$

which we refer to as a “Coxeter presentation”. This is recorded in the graph Figure 1, which has a single line for each power 3 in the relations (we do not record the commuting cases, in which the powers are equal to 2). Given a word $\underline{w} = s_{i_1} s_{i_2} \dots s_{i_\ell}$ in these generators, we define the length of \underline{w} to be ℓ .

We refer to any subgroup corresponding to a subset of the generators as a **parabolic subgroup**. Our favourite parabolic is $\mathfrak{S}_k \times \mathfrak{S}_{n-k} \leq \mathfrak{S}_n$.

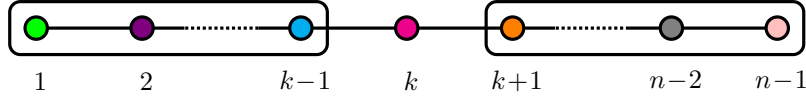


FIGURE 1. The parabolic Coxeter diagram for $\mathfrak{S}_k \times \mathfrak{S}_{n-k} \leq \mathfrak{S}_n$.

The easiest (non-trivial) example of Kazhdan–Lusztig theory is given by considering the parabolic Coxeter system $\mathfrak{S}_k \times \mathfrak{S}_{n-k} \leq \mathfrak{S}_n$. In this lecture we will illustrate how one can understand this combinatorially.

1.2. A Bruhat graph. By a number line we mean a horizontal line containing some vertices indexed by the integers $1, \dots, n$ in increasing order from left to right. A weight is a diagram obtained by labelling each of the vertices on such a number line by \vee (down), \wedge (up). We define an (n, k) -configuration to be a collection of k uparrows and $(n - k)$ downarrows attached to the numberline at the points $1, \dots, n$ and denote the set of all such configurations by $\Lambda_{n,k}$. It is easy to see that \mathfrak{S}_n acts on the set of all possible (n, k) -configurations. We draw an initial configuration by putting k uparrows on the points $1, \dots, k$ followed by $(n - k)$ downarrows on the points $k + 1, \dots, n$ to obtain a diagram. See Figure 2 for an example. We denote the initial configuration by \emptyset . The stabiliser of the initial configuration is given by $\mathfrak{S}_k \times \mathfrak{S}_{n-k} \leq \mathfrak{S}_n$

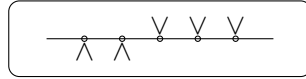


FIGURE 2. An initial configuration for $n = 5$ and $k = 2$.

Definition 1.1. The Bruhat graph for $\mathfrak{S}_k \times \mathfrak{S}_{n-k} \leq \mathfrak{S}_n$ is given as follows:

- start by drawing the initial configuration at the bottom.
- If applying a simple reflection does result in a new weight, then record this in the next level up in the diagram. We record the colour of the reflection as an edge relating the two points in the graph.

We repeat the above until the process terminates.

This is best illustrated via the example in Figure 3.

Definition 1.2. We define the Bruhat order as follows. We write $\lambda < \mu$ if λ contains strictly fewer \wedge arrows than μ . If λ has the same number of \wedge arrows (and therefore the same number of \vee arrows) as μ then we write $\lambda < \mu$ if there's a bijection between the \wedge arrows (respectively \vee arrows) of λ and those of μ such that each \wedge arrow (respectively \vee arrow) in λ appears further to the left (respectively right) than the corresponding one in μ . We write w_λ^μ for any such permutation of minimal length.

The element w_λ^μ is, in fact, unique and can be constructed in an elementary fashion as follows. First draw $\lambda \in \Lambda_{n,k}$, along a horizontal numberline and μ along a parallel numberline. Then connect the i th \vee along the bottom edge to the i th \vee along the top edge for $1 \leq i \leq k$ and similarly for the up arrows. In the case that λ (respectively μ) is the unique minimal (respectively maximal) weight in $\Lambda_{n,k}$ with all up arrows drawn to the left (respectively right) we set $w_0 := w_\lambda^\mu$ and refer to this as the longest coset in $\Lambda_{n,k}$. We note that for λ minimal, μ maximal and ν arbitrary $w_0 = w_\lambda^\nu w_\nu^\mu$. The longest coset in $\Lambda_{n,k}$ can be thought of as the $(k \times (n - k))$ -rectangular permutation as illustrated in Figure 4. With this rectangular visualisation in place it is clear that we can have a bijection between $\{w_\alpha^\beta \mid \alpha, \beta \in \Lambda_{n,k}, \alpha < \beta\}$ and skew partitions which fit into a $(k \times (n - k))$ -rectangle. We depict the rectangular region

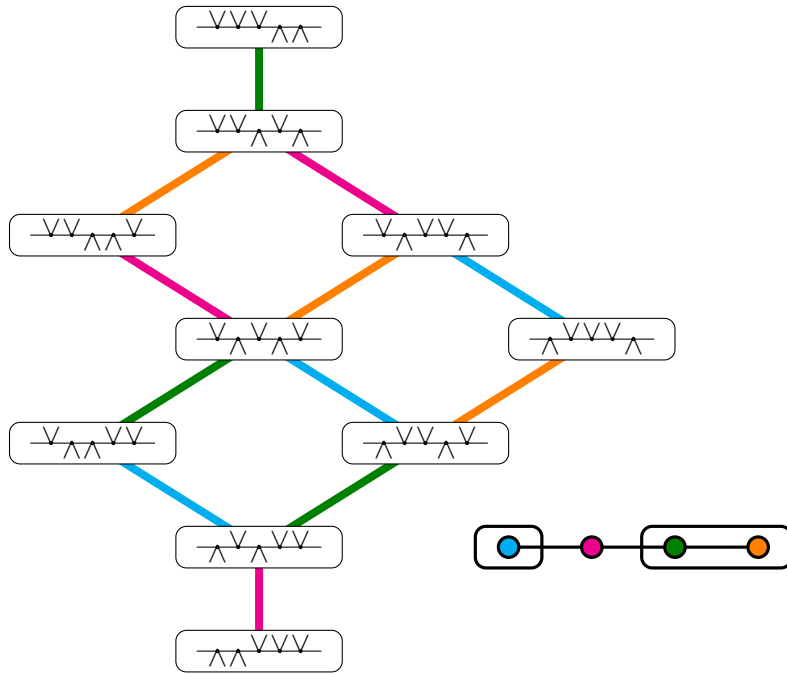


FIGURE 3. The Bruhat graph for $\mathfrak{S}_2 \times \mathfrak{S}_3 \leq \mathfrak{S}_5$.

and tilings of this region (in the sense of Young diagrams) and as in Figure 14. We will freely label weights by the up-down arrow diagrams or by their corresponding partitions, as is deemed convenient.

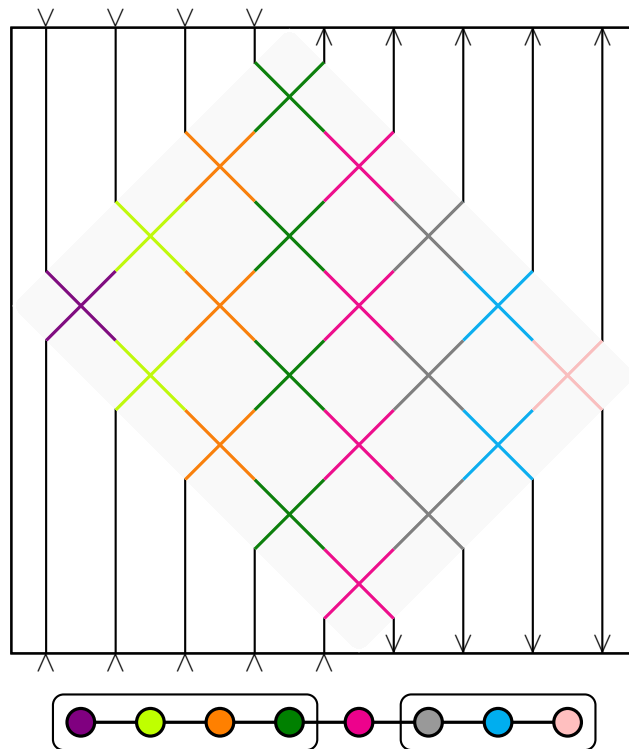


FIGURE 4. The longest coset in $\Lambda_{9,5}$.

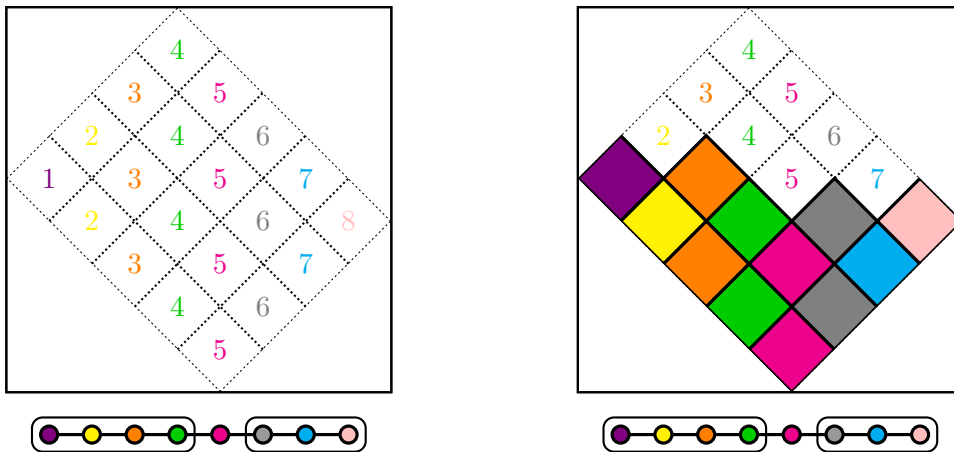


FIGURE 5. On the left we depict the (5×4) -rectangle in which we embed $\Lambda_{9,5}$. On the right we draw an element $\lambda \in \Lambda_{9,5}$ as a partition.

We say that a pair of tiles within the $(k \times (n - k))$ -rectangle are **neighbouring** if they meet at an edge (which necessarily has an angle of 45° or 135°). Given a pair of neighbouring tiles X and Y , we say that Y **supports** X if X appears above Y . We say that a tile, X , is **fully supported** if every tile within the $(k \times (n - k))$ -rectangle which can support X does support X . We say that a collection of tiles, λ is a **partition** if every tile in λ is fully supported. We depict a partition λ by colouring the tiles of λ . Given $\mu \in \Lambda_{n,k}$ a partition, we define the set of all **addable** tiles, $\text{Add}(\mu)$, to be the tiles X such that $\mu + X$ is a partition; similarly, we define the set of all **removable** tiles, $\text{Rem}(\mu)$, to be the tiles Y such that $\mu - Y$ is a partition.

1.3. Paths in our Bruhat graph. We now introduce graded paths in the Bruhat graph and use these to define the Kazhdan–Lusztig polynomials.

Definition 1.3. For each edge of $\lambda \rightarrow \mu$ the Bruhat graph, we allow it to be traversed in four possible ways. These paths are as follows,

- (U) The ‘up’ move, $\lambda \rightarrow \mu$, of degree 0;
- (UD) The ‘up-down’, $\lambda \rightarrow \lambda$, of degree 1;
- (DU) The ‘down-up’, $\mu \rightarrow \mu$, of degree -1 ;
- (D) The ‘down’, $\mu \rightarrow \lambda$, of degree 0.

Definition 1.4. Let $\lambda, \nu \in \Lambda_{n,k}$. We define a path, \mathbb{T} , of shape $\nu \setminus \lambda$ and length ℓ to be a sequence

$$\lambda = \lambda^{(0)} \rightarrow \lambda^{(1)} \rightarrow \dots \rightarrow \lambda^{(\ell)} = \nu$$

in the Bruhat graph. We let $\text{Path}(\nu)$ denote the set of all paths from the identity to the point ν in the Bruhat graph. Given $\mathbb{T} \in \text{Path}(\nu)$, we write $\text{Shape}(\mathbb{T}) = \nu$ and say the path has shape equal to ν .



FIGURE 6. An example of a path, \mathbb{S} , of length 3. We record the direction in which we travel along the coloured edge in each step in the path. This path has degree 1.

Definition 1.5. We say that a path $\mathbb{T}^\mu \in \text{Path}(\mu)$ is **reduced** if it is a path of shortest possible length from the identity to μ .



FIGURE 7. An example of a reduced path \mathbb{T}^μ . We travel upwards along each coloured edge in each step in the path. This path has degree 0.

Remark 1.6. We remark that reduced paths in $\text{Path}(\mu)$ can be identified with the classical definition of standard Young paths of shape μ via the rectangular visualisation.

Exercise 1.7. Calculate the number of distinct reduced words for $w_0 \in \Lambda_{5,2}$.

By picking a fixed reduced path, $\mathbb{T}^\mu \in \text{Path}(\mu)$, we are able to consider all possible paths with the same colour sequence as \mathbb{T}^μ but which terminate at another point λ . For a fixed λ , we denote the set of all such paths by $\text{Path}(\lambda, \mathbb{T}^\mu)$.

Example 1.8. Let $n = 5$ and $k = 2$. We consider the weights

$$\lambda = \boxed{\begin{array}{ccccccc} & & \vee & \vee & & \vee & \\ \wedge & & & & \wedge & & \vee \end{array}} \quad \mu = \boxed{\begin{array}{ccccccc} \vee & & \vee & & \vee & & \vee \\ & \wedge & & \wedge & & \wedge & \end{array}}.$$

If we set \mathbb{T}^μ be the reduced path depicted in Figure 7, then we note that the path \mathbb{S} depicted in Figure 6 belongs to $\text{Path}(\lambda, \mathbb{T}^\mu)$.

We are now ready to define the Kazhdan–Lusztig polynomials in terms of walks in the Bruhat graph. This will allow us to provide a closed combinatorial description of these polynomials later in the lecture.

Definition 1.9. The antispherical Kazhdan–Lusztig polynomials, $n_{\lambda,\mu}(q)$, associated to the parabolic Coxeter system $\mathfrak{S}_k \times \mathfrak{S}_{n-k} \leq \mathfrak{S}_n$ are defined as follows

$$n_{\lambda,\mu}(q) = \sum_{\mathbb{S} \in \text{Path}(\lambda, \mathbb{T}^\mu)} q^{\deg(\mathbb{S})}$$

for $\lambda, \mu \in \Lambda_{n,k}$ and any choice of reduced path \mathbb{T}^μ .

We will provide a closed combinatorial formula for these Kazhdan–Lusztig polynomials later in the lecture. This will make clear a number of properties which are not at all obvious from the definition above. For instance these polynomials are all monic (they evaluate to 1 when $q = 1$) but this is not at all obvious from Definition 1.9.

Remark 1.10. The definition above masks the real difficulty of calculating Kazhdan–Lusztig polynomials. This is because the case $\mathfrak{S}_k \times \mathfrak{S}_{n-k} \leq \mathfrak{S}_n$ is much easier than the general case. However, it will serve as our first step toward understanding the general picture, which we will discuss shortly.

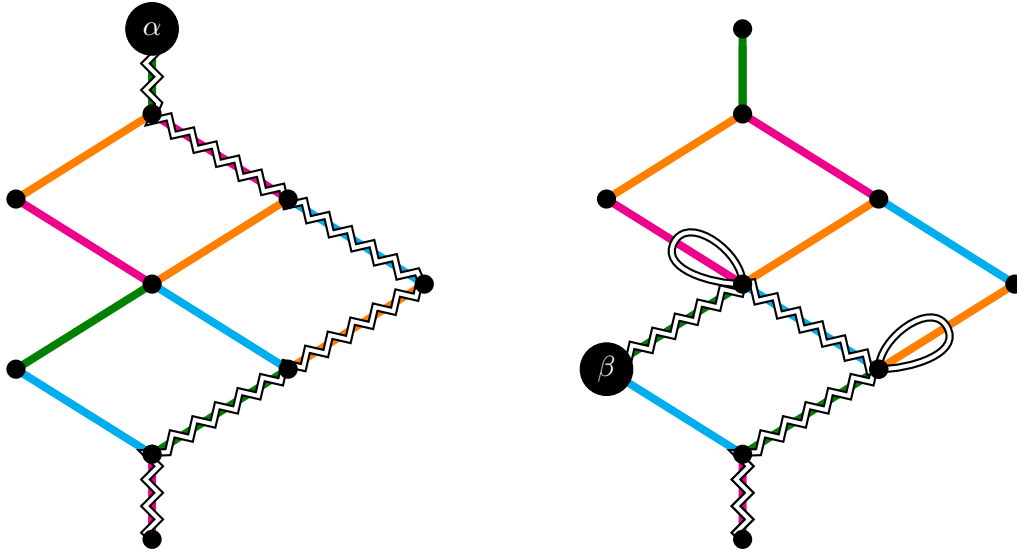


FIGURE 8. On the left we depict a path T^α and on the right we depict the unique element of $\text{SStd}(\beta, T^\alpha)$ for $\alpha = (2^3), \beta = (2) \in \Lambda_{5,2}$. We have that $n_{\beta,\alpha}(q) = q^2$.

Exercise 1.11. Calculate the complete (10×10) -table of all antispherical Kazhdan–Lusztig polynomials for the parabolic Coxeter system $\mathfrak{S}_2 \times \mathfrak{S}_3 \leq \mathfrak{S}_5$.

1.4. Temperley–Lieb combinatorics. Temperley–Lieb diagrams provide the quantum combinatorics we will need in order to provide a simple closed combinatorial formula for our Kazhdan–Lusztig polynomials.

Definition 1.12. Let W be a Coxeter group of rank n . The Temperley–Lieb monoid of type W is the algebra, TL_W , generated by E_i for $1 \leq i \leq n$ subject to the relations

$$\underbrace{E_i E_j \dots}_{m_{ij}} = \underbrace{E_i E_j \dots}_{m_{ij}-2} \tag{1.1}$$

for $m_{ij} > 2$ and the relations

$$E_i^2 = E_i \quad E_i E_j = E_j E_i \tag{1.2}$$

for $m_{ij} = 2$.

Remark 1.13. We have a surjective homomorphism $\mathbb{k}W \rightarrow \text{TL}_W$ given by

$$\frac{1}{2}(1 + s_i) \mapsto E_i$$

providing the field is of odd characteristic.

For W the symmetric group, there is a simple and intuitive way to visual the elements of this algebra, as follows.

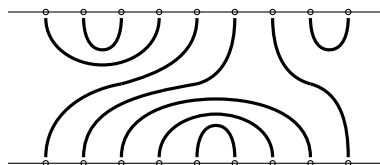


FIGURE 9. A Temperley–Lieb diagram.

Definition 1.14. An n -strand Temperley-Lieb diagram is a frame with n vertices on the top and bottom which are paired-off by n non-crossing strands. We refer to a strand connecting a top and bottom vertex as a propagating strand. We refer to any strand connecting to top vertices (or two bottom vertices) to each other as an arc. We define E_i to be the diagram with a single pair of arcs connecting the i th and $(i + 1)$ th northern (respectively southern) vertices, and with $(n - 2)$ vertical strands.

Definition 1.15. An (n, k) -orientation on a Temperley-Lieb diagram is a pair of weights $\lambda, \mu \in \Lambda_{n,k}$ on the top and bottom edges such that the arrows on a propagating strand match, whereas the arrows on an arcs are opposites of each other. We define the degree of an oriented Temperley-Lieb diagram to be given by

$$\#\{\text{clockwise oriented northern arcs}\} - \#\{\text{anti-clockwise oriented southern arcs}\}. \quad (1.3)$$

Remark 1.16. We remark that and Temperley-Lieb diagram whose bottom weight is provided by \emptyset has manifestly non-negative degree (all southern arcs are clockwise oriented). These are the diagrams which will be used to calculate Kazhdan-Lusztig polynomials. Moreover, we now have a closed (i.e. non-iterative) definition of the degree.

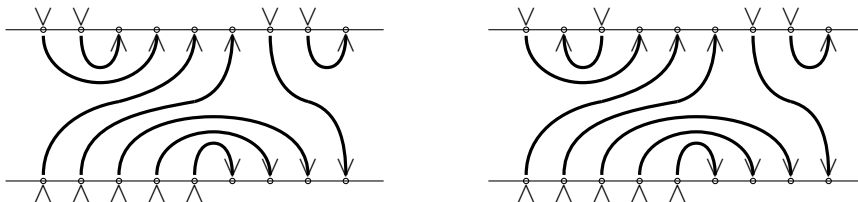


FIGURE 10. A pair of oriented Temperley-Lieb diagrams. The tilings for these diagrams are given in Figure 14.

Definition 1.17. Let $\lambda \leq \mu$ and suppose that $\lambda \xrightarrow{s_i} \mu$ is a traversal of an edge in the Bruhat graph. The corresponding oriented Temperley-Lieb diagram, $E_{\lambda \rightarrow \mu}^i$ is obtained by placing the weight λ along the bottom, the weight μ along the top, and then placing the corresponding the Temperley-Lieb generator E_i in between the two weights. Given $\mathsf{T} \in \text{Path}(\lambda)$ a path

$$\emptyset = \lambda^{(0)} \xrightarrow{i_1} \lambda^{(1)} \xrightarrow{i_2} \dots \xrightarrow{i_\ell} \lambda^{(\ell)} = \lambda$$

we define

$$E_{\mathsf{T}} = E_{\lambda^{(0)} \rightarrow \lambda^{(1)}}^{i_1} E_{\lambda^{(1)} \rightarrow \lambda^{(2)}}^{i_2} \dots E_{\lambda^{(\ell-1)} \rightarrow \lambda^{(\ell)}}^{i_\ell}.$$

Example 1.18. Let's consider the edge $\lambda \xrightarrow{s_3} \mu$ in Figure 3 for

$$\lambda = \boxed{\begin{array}{c} \text{---} \bigvee \text{---} \bigvee \bigvee \text{---} \\ \bigwedge \quad \bigwedge \quad \bigwedge \end{array}} \quad \mu = \boxed{\begin{array}{c} \text{---} \bigvee \bigvee \bigvee \text{---} \\ \bigwedge \quad \bigwedge \quad \bigwedge \end{array}}$$

The four possible traversals of this edge correspond to the Temperley-Lieb-style elements depicted in Figure 11 and are of degrees $-1, 0, 0,$ and 1 respectively.

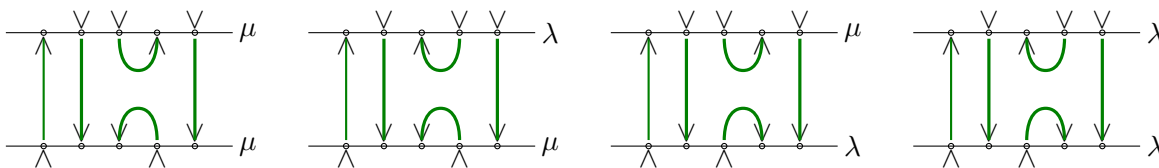


FIGURE 11. Let λ and μ be as in Example 1.18. We picture the four Temperley-Lieb diagrams associated to the edge $\lambda \xrightarrow{s_3} \mu$.

We often compress the step-by-step construction of a Temperley–Lieb diagram into the same “rectangular form” as we did with cosets. An example of this can be seen in Figure 14.

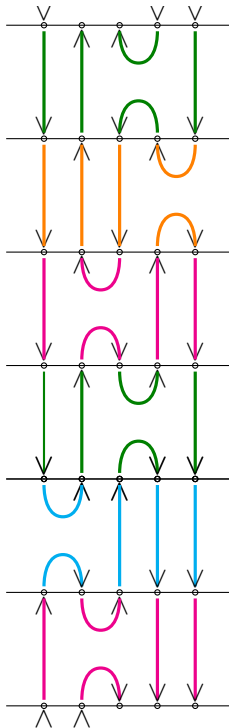


FIGURE 12. The Temperley–Lieb diagram of shape $\lambda = (2)$ and weight $\mu = (2^3)$; reading from bottom-to-top, the diagrams have degree 0, 0, 0, 1, 1, and 0 respectively.

Given $\mathsf{T}^\mu \in \text{Path}(\mu)$ a reduced path, the diagram E_{T^μ} is of degree zero (all north-ern/souther arcs are anti-clockwise/clockwise oriented) and is independent of the choice of reduced path. We let e_μ denote the Temperley–Lieb diagram obtained by forgetting the weights of the diagram E_{T^μ} . The top half of the diagram e_μ is the cup-diagram obtained by connecting up and down arrows by clockwise oriented cups (according to the usual rule for nested parentheses) where possible, and adding rays at all unjoined arrows.

Given $\lambda, \mu \in \Lambda_{n,k}$ we define λe_μ to be the diagram obtained from placing the weight λ (respectively the weight \emptyset) on top of (respectively the bottom of) the diagram e_μ , if the resulting diagram is oriented. If the diagram is not oriented, we leave λe_μ undefined.

Example 1.19. *The diagram $E_{\mathsf{T}^{(5^2,1^2)}}$ is pictured on the left of Figure 14 and the diagram $e_{(5^2,1^2)}$ is pictured in Figure 9. The diagram $(4,3,1^2)e_{(5^2,1^2)}$ is pictured on the right of Figure 9 and it has degree 2 (equal to the number of clockwise oriented arcs).*

Exercise 1.20. *The full matrix of Kazhdan–Lusztig polynomials for $\mathfrak{S}_2 \times \mathfrak{S}_2 \leq \mathfrak{S}_4$ is depicted in Figure 13. The columns are labelled by the top half of the diagram e_μ ; the rows are labelled by the corresponding λ . Verify this calculation by drawing λe_μ in each case. That is, place the weight λ on top half of e_μ and check the degree of this half diagram.*

Exercise 1.21. *Calculate the full matrix of Kazhdan–Lusztig polynomials for $\mathfrak{S}_2 \times \mathfrak{S}_3 \leq \mathfrak{S}_5$*

	1
	q	1
	.	q	1	.	.	.
	.	q	.	1	.	.
	q	q^2	q	q	1	.
	q^2	.	.	.	q	1

FIGURE 13. The Kazhdan-Lusztig polynomials $n_{\lambda,\mu}(q)$ for $\mathfrak{S}_2 \times \mathfrak{S}_2 \leq \mathfrak{S}_4$.

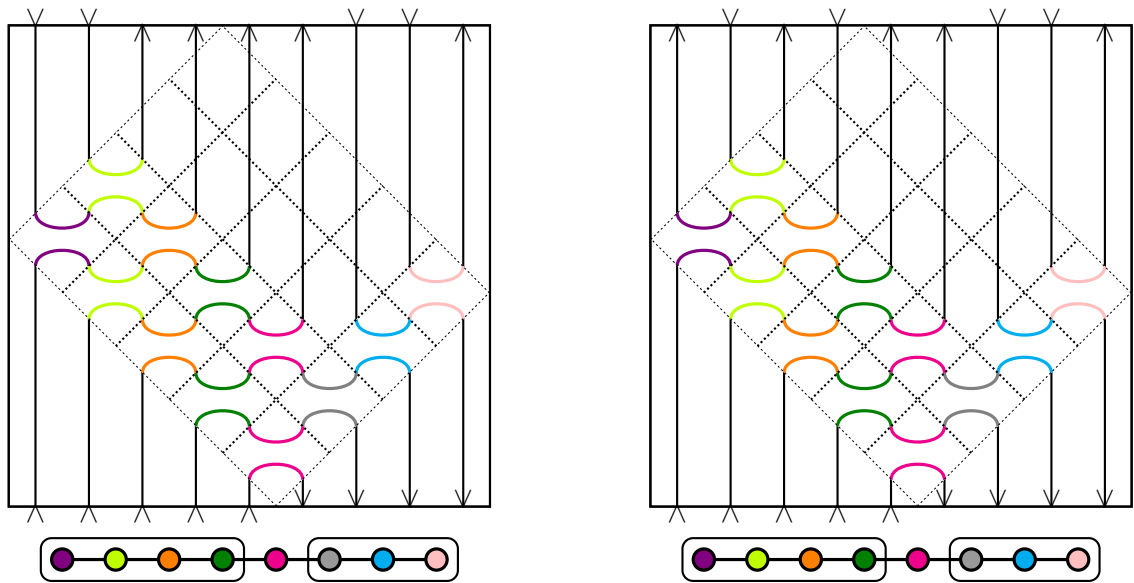


FIGURE 14. The tilings of two oriented Temperley-Lieb diagrams. The former diagram is $E_{\top(5^2,1^2)}$. The latter diagram is E_S for $S \in \text{Path}((4,3,1^2), \top(5^2,1^2))$. The latter diagram is obtained by reorienting the topmost orange tile of the former.

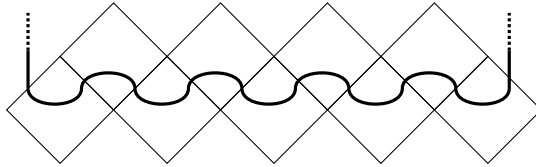
Theorem 1.22. *The antispherical Kazhdan-Lusztig polynomials, $n_{\lambda,\mu}(q)$, associated to the parabolic Coxeter system $\mathfrak{S}_k \times \mathfrak{S}_{n-k} \leq \mathfrak{S}_n$ can be calculated explicitly as follows:*

$$n_{\lambda,\mu}(q) = \begin{cases} q^{\deg(\lambda e_\mu)} & \text{if } \lambda e_\mu \text{ is defined} \\ 0 & \text{otherwise} \end{cases}$$

Proof. Any oriented Temperley-Lieb diagram λe_μ can be constructed iteratively in terms of its rectangular tiling (and vice versa). Therefore the set of oriented Temperley-Lieb diagrams

of shape λ and weight μ is in bijection with $\text{Path}(\lambda, \mathbb{T}^\mu)$. By construction the former set has at one element (if λe_μ is oriented) or is empty.

It remains to show that $\deg(\mathbf{S}) = \deg(\lambda e_\mu)$ for $\mathbf{S} \in \text{SStd}(\lambda, \mathbb{T}^\mu)$. We first observe that the degree of generator diagram $E_{\lambda \rightarrow \mu}^i$ is equal to the corresponding degree of the path $\lambda \rightarrow \mu$ as defined in Definition 1.3. It remains to consider an arbitrary oriented Temperley–Lieb diagram, which we will reduce to the generator case using the tilings picture. Any northern arc in a Temperley–Lieb diagram passes through an odd number of tiles. In fact the set of tiles is a “wiggle” of the form



Reading from left to right, the strand oscillates between being either the “top” or “bottom” of a given Temperley–Lieb generator tile. Assume the arc is clockwise-oriented. We count the degree using the definition for each $E_{\lambda \rightarrow \mu}^i$ (which matches the degree on paths). The degree contribution as it passes through these tiles is given by

$$+1 - 1 + 1 - 1 + 1 - 1 \cdots + 1 = 1$$

by equation (1.3) (notice that the strand is locally either a clockwise northern arc or an anticlockwise southern arc at each step). If the arc is anti-clockwise oriented then it has degree $0 + \cdots + 0 = 0$. Thus the degrees match up. One can repeat this exercise with each southern arc and propagating strand in the diagram (although we remark that these contributions are all zero and this is less interesting). \square

1.5. The general framework. Lie theorists are generally nowadays mostly interested in Kazhdan–Lusztig polynomials for infinite groups. Foremost of which is the affine or cylindrical symmetric group $\widehat{\mathfrak{S}}_n$. This group consists of the monomial matrices with entries t^i for some formal variable t and $i \in \mathbb{Z}$, for example

$$\begin{pmatrix} 0 & 0 & 1 & 0 & 0 & 0 \\ t^2 & 0 & 0 & 0 & 0 & 0 \\ 0 & 0 & 0 & 1 & 0 & 0 \\ 0 & 0 & 0 & 0 & t^{-1} & 0 \\ 0 & 1 & 0 & 0 & 0 & 0 \\ 0 & 0 & 0 & 0 & 0 & 1 \end{pmatrix} \in \widehat{\mathfrak{S}}_6$$

We picture elements of $\widehat{\mathfrak{S}}_n$ as strand-diagrams on a cylinder, decorated with a dashed “border” as a reference point on the cylinder as in Figure 15.

If a strand from the i th to the j th position crosses the border in the clockwise (respectively anti-clockwise) direction a total of x times, then we place the entry q^x (respectively q^{-x}) in the intersection of row i and column j . Any diagram/matrix is a product of the usual elements $(i, i+1)$ drawn so that they do not cross the dashed border (whose matrix coefficients are only equal to 0 or 1) together with the diagram/matrix depicted in Figure 15. The affine symmetric group has Coxeter presentation

$$\widehat{\mathfrak{S}}_n = \langle s_i, 1 \leq i \leq n \mid s_i^2 = 1, (s_i s_{i+1})^3 = 1, (s_n s_1)^3 = 1, \text{ and } (s_i s_j)^2 = 1 \text{ otherwise} \rangle.$$

For example, the representation theory of general linear group of $(h \times h)$ -matrices is controlled by the Kazhdan–Lusztig polynomials of the parabolic Coxeter system of type $\mathfrak{S}_n \leq \widehat{\mathfrak{S}}_n$.

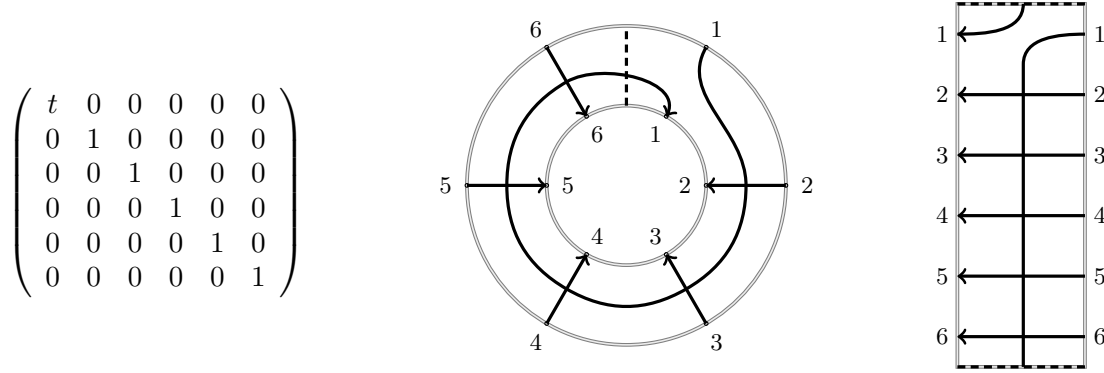


FIGURE 15. An element of $\widehat{\mathfrak{S}}_6$, three ways. The former diagram is the projection of the cylinder into the plane. In the latter we glue the two dashed edges of the rectangular diagram together to obtain the cylinder.

Exercise 1.23. Write the affine Coxeter generator s_n as an $(n \times n)$ -monomial matrix.

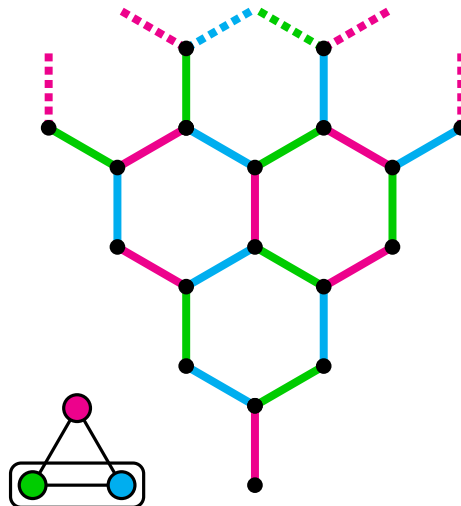


FIGURE 16. The Bruhat graph for $\mathfrak{S}_3 \leq \widehat{\mathfrak{S}}_3$. This graph can be thought of as a hexagonal-tiling of a sixth of the plane.

We can generalise all the ideas of our previous sections generalise to the setting of a parabolic subgroup P of a Coxeter group W . Of our three definitions of weight (via up-down diagrams, cosets, and partitions) the only definition that generalises directly is that of cosets. The path combinatorics passes through verbatim, but our Temperley-Lieb calculus does not. The Bruhat order can no longer be visualised in terms of weights, but can be in terms of (sub)words in the Coxeter generators.

Our Temperley-Lieb combinatorics of the previous sections allowed us to show that any non-reduced path in the Bruhat graph of $\mathfrak{S}_k \times \mathfrak{S}_{n-k} \leq \mathfrak{S}_n$ is manifestly positive. This is seldom true in general. For example, in $\mathfrak{S}_3 = \langle s_1, s_2 \mid (s_1 s_2)^3 = 1, s_i^2 = 1 \rangle$ we have two paths of shape s_1 and weight $s_1 s_2 s_1$. To see this, we define T^μ to be the path

$$\emptyset \xrightarrow{U} s_1 \xrightarrow{U} s_1 s_2 \xrightarrow{U} s_1 s_2 s_1$$

and we note that the two elements of $\text{Path}(s_1, T^{s_1 s_2 s_1})$ are as follows,

$$\emptyset \xrightarrow{U} s_1 \xrightarrow{UD} s_1 \xrightarrow{DU} s_1 \quad \emptyset \xrightarrow{UD} \emptyset \xrightarrow{UD} \emptyset \xrightarrow{U} s_1$$

which have degrees 0 and 2 respectively. The path of degree 0 does not contribute to the Kazhdan–Lusztig polynomial which is $n_{s_1, s_1 s_2 s_1} = q^2$. This is essentially the only added complexity: we must remove patterns in the Kazhdan–Lusztig polynomials which arise from polynomials in $\mathbb{N}[q + q^{-1}]$. This can be seen as a shadow of the fact that Kazhdan–Lusztig theory controls the graded Loewy structure of algebra modules.

Definition 1.24. We recursively define polynomials

$$b_{\lambda, \mu}(q) \in \mathbb{Z}[q + q^{-1}] \quad n_{\lambda, \mu}(q) \in \mathbb{Z}[q]$$

by induction on the Bruhat order \leq as follows

$$b_{\lambda, \mu}(q) + n_{\lambda, \mu}(q) = \sum_{S \in \text{Path}(\lambda, T^\mu)} q^{\deg(S)} - \sum_{\lambda < \nu < \mu} b_{\nu, \mu}(q) n_{\lambda, \nu}(q). \quad (1.4)$$

Remark 1.25. We outline the construction in a little more detail. The righthand-side of equation (1.4) is calculated by induction. The resulting polynomial will, in general, have some terms of the form $\alpha_i q^{-i}$ for $i \geq 0$ and we group together these terms (along with their twins $\alpha_i q^i$ for $i > 0$) in order to form the polynomial $b_{\lambda, \mu}(q)$. The remaining terms are all of strictly positive degree and these are grouped together to form $n_{\lambda, \nu}(q)$.

Example 1.26. The subtracted term is zero for $\lambda = \mu$ or λ and μ adjacent in the Bruhat order. There is a single element of $\text{Path}(\lambda, T^\mu)$ of degree 0 or 1 respectively in these cases. Therefore

$$b_{\lambda, \lambda}(q) = 1 \quad n_{\lambda, \lambda} = 1 \quad b_{\lambda, \mu}(q) = 0 \quad n_{\lambda, \mu}(q) = q$$

for $\mu < \lambda$ adjacent in the Bruhat order.

Example 1.27. For $\mathfrak{S}_k \times \mathfrak{S}_{n-k} \leq \mathfrak{S}_n$ we have that $b_{\lambda, \mu}(q) = 0$ for all λ, μ and this is part of the reason why these polynomials were so easy to compute.

Example 1.28. We record the polynomials $b_{\nu, \mu}(q)$ and $n_{\lambda, \nu}(q)$ for \mathfrak{S}_3 in the tables in Figures 17 and 18. Multiplying these matrices together we obtain the matrix with entries given by $\sum_{S \in \text{Path}(\lambda, T^\mu)} q^{\deg(S)}$.

	\emptyset	s_1	s_2	$s_1 s_2$	$s_2 s_1$	$s_1 s_2 s_1$
\emptyset	1
s_1	q	1
s_2	q	.	1	.	.	.
$s_1 s_2$	q^2	q	q	1	.	.
$s_2 s_1$	q^2	q	q	.	1	.
$s_1 s_2 s_1$	q^3	q^2	q^2	q	q	1

FIGURE 17. The polynomials $n_{\lambda, \mu}(q)$ for \mathfrak{S}_3

	\emptyset	s_1	s_2	$s_1 s_2$	$s_2 s_1$	$s_1 s_2 s_1$
\emptyset	1
s_1	.	1
s_2	.	.	1	.	.	.
$s_1 s_2$.	.	.	1	.	.
$s_2 s_1$	1	.
$s_1 s_2 s_1$.	1	1	.	.	1

FIGURE 18. The polynomials $b_{\lambda, \mu}(q)$ for \mathfrak{S}_3

Exercise 1.29. Calculate the Kazhdan–Lusztig polynomials for \mathfrak{S}_4 .

Exercise 1.30. Calculate the first few examples of $n_{\lambda,\mu}(q)$ for $\mathfrak{S}_3 \leq \widehat{\mathfrak{S}}_3$.

Remark 1.31. It is not clear that the polynomials defined in Definition 1.24 have non-negative coefficients for a given Coxeter group W . This was the subject of the Kazhdan-Lusztig positivity conjecture. This conjecture was proven using the diagrammatic Hecke category \mathcal{H}_W by interpreting the polynomials $b_{\lambda,\mu}(q)$ as the graded characters of simple \mathcal{H}_W -modules and the $n_{\lambda,\mu}(q)$ as the graded composition multiplicities of simple modules in Verma modules for \mathcal{H}_W .

2. THE DIAGRAMMATIC HECKE CATEGORY FOR $\mathfrak{S}_k \times \mathfrak{S}_{n-k} \leq \mathfrak{S}_n$

We will first introduce the Soergel diagrams in terms of morphisms between paths within the Bruhat graph $P = \mathfrak{S}_k \times \mathfrak{S}_{n-k} \leq \mathfrak{S}_n = W$. We will then define the diagrammatic Hecke category as the span of Soergel diagrams modulo certain relations. We will then construct a \mathbb{Z} -basis of the diagrammatic Hecke category and use this to construct the projective, simple, and Verma modules. We will also be able to calculate the full Loewy structure of Verma modules. In the next section we will consider more general parabolic Coxeter systems (W, P) .

2.1. Morphisms between paths. We wish to consider all possible ways of deforming one path into another. We will see that there are precisely four “generator” morphisms (identity, spot, fork, and braid) and that all other morphisms can be written as repeated applications of these. The spot and fork morphisms allow us to shrink and grow paths; the braid morphism allows us to bend a path around the perimeter of a $2m$ -gon in the Bruhat graph. The only $2m$ -gons in the Bruhat graph for $P = \mathfrak{S}_k \times \mathfrak{S}_{n-k} \leq \mathfrak{S}_n = W$ are squares (notice that \mathfrak{S}_3 and its affinizations have hexagons in the Bruhat graph) — this makes the situation simpler.

Each σ -edge in the Bruhat graph has an identity morphism to itself, which we denote by 1_σ . We record the colour of the edge along the top and bottom of a rectangular frame and join these colourings by a single vertical strand. Each reduced path T has an identity morphism to itself (denoted by 1_T) which we obtain by horizontally concatenating (denoted \otimes) the identity morphism for each edge traversed by the path as depicted in Figure 19. We also have the a map from the empty path to itself, which we represent by an empty frame.

FIGURE 19. The identity morphism for the path T^α depicted in Figure 8.

Notation 2.1. Let $\sigma \in \text{Rem}(\lambda)$. We let T^λ denote any reduced path of shape λ ; we let $T^{\lambda-\sigma}$ denote the reduced path of shape $\lambda - \sigma$ obtained by deleting the final occurrence of σ . We define $\text{braid}_{T^\lambda}^{T^{\lambda-\sigma} \otimes T^\sigma}$ to be the minimal length colour-preserving bijection between these paths.

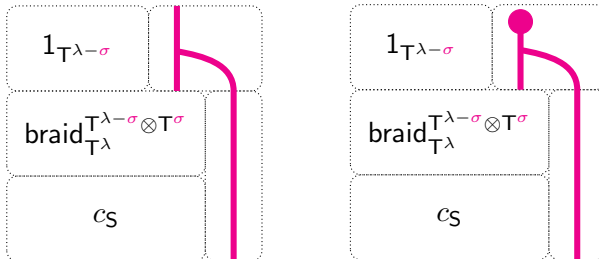
FIGURE 20. Examples of braid elements. We remark that the intersecting pairs of strands are labelled by pairs of commuting reflections in the Coxeter graph.

We can view a path $S \in \text{Path}(\lambda, T^\mu)$ as a morphism, c_S , from a reduced path T^μ to a reduced path T^λ as follows. We grow the top and bottom labelling of the frame according to the shape and weight of S respectively. We proceed by induction, we suppose that $S \in \text{Path}(\lambda, T^\mu)$ and that the next step in the path has colour σ . There are four cases (corresponding to the four possible traversals of an edge) to consider.

- Suppose $\sigma \in \text{Add}(\lambda)$. For a U step we draw a vertical strand; for an UD step we draw a vertical strand from the bottom of the diagram terminating at a spot in the middle of the diagram. Thus obtaining

respectively.

- Suppose $\sigma \in \text{Rem}(\lambda)$. We first apply the braid element to c_S in order to obtain a diagram whose final colour on the northern edge of the frame is σ . For a DU step we connect the penultimate σ -strands in $c_S \otimes 1_\sigma$ with a fork. For a D step we connect the penultimate σ -strands in $c_S \otimes 1_\sigma$ and then place a dot on top of this strand. Thus obtaining



respectively. We note that the actual final strand of c_S may

We define $c_{S\uparrow} = c_S^* c_\uparrow$ where $*$ denotes the diagram obtained by flipping through the horizontal axis. An example is given in Figure 21.

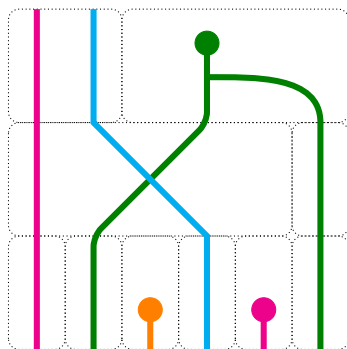


FIGURE 21. The element c_S constructed from the path S in Figure 8.

Exercise 2.2. Construct all path-morphisms indexed by elements of $\text{Path}(\lambda, T^\mu)$ for $\lambda \in \Lambda_{5,2}$ and T^μ the leftmost path in Figure 8.

We remark that every local region of a path-morphism diagram is a strand, fork, spot, or a braid. We define a Soergel diagram to be any diagram whose local neighbourhoods are all of this form. We will define the diagrammatic Hecke category, $\mathcal{H}_{P \setminus W}$, to be the span of all path-morphisms with multiplication given by vertical concatenation modulo certain relations (S1) to (S7) which we will slowly introduce (and motivate) over the next few subsections.

We define the graded degree of a spot generator to be $+1$ and that of the fork generator to be -1 . All other regions of a Soergel diagram have degree 0 . We remark that this is consistent with the definition of the degree of a path (and the construction of path-morphisms).

2.2. The Hecke category. We first introduce the one colour relations. This allows us to discuss the representation theoretic structure of the Hecke category of \mathfrak{S}_2 in great detail. This is intended to warm-up the reader to the ideas we will see later on. The one colour local relations in the Hecke category are as follows

together with the “one colour Demazure” relation

$$\begin{array}{|c|} \hline \bullet \\ \hline \bullet \\ \hline \end{array} = 2 \begin{array}{|c|} \hline \bullet \\ \hline \bullet \\ \hline \end{array} - \begin{array}{|c|} \hline \bullet \\ \hline \bullet \\ \hline \end{array} \tag{S2}$$

and their vertical and horizontal flips. Finally, we have the non-local (one colour) cyclotomic relation

$$\begin{array}{|c|} \hline \bullet \\ \hline \bullet \\ \hline \end{array} \otimes 1_S = 0 \tag{S3}$$

for $\sigma \in W$ and S an arbitrary path. One can, roughly speaking, think of these relations as ensuring that there is a unique one colour diagram in each degree of the grading.

Example 2.3. *The Bruhat graph for $W = \mathfrak{S}_2$ consists of two vertices labelled by the identity and the transposition $(1, 2) \in \mathfrak{S}_2$ (or equivalently the corresponding weight labels from the previous section) which are connected by a single edge.*

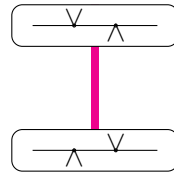


FIGURE 22. The Bruhat graph for $W = \mathfrak{S}_2$. One can regard the parabolic as being the trivial subgroup $P = \mathfrak{S}_1 \times \mathfrak{S}_1$.

There are precisely two reduced paths T^\emptyset and $T^{(1,2)}$. We have that $\text{SStd}(\lambda, T^\emptyset)$ is non-empty only if $\lambda = \emptyset$, in which case it consists of the empty path T^\emptyset . The elements of $\text{SStd}(\lambda, T^{(1,2)})$ are as follows

$$\begin{array}{|c|} \hline \wedge \\ \hline \vee \\ \hline \end{array} \xrightarrow{U} \begin{array}{|c|} \hline \vee \\ \hline \wedge \\ \hline \end{array} \qquad \begin{array}{|c|} \hline \wedge \\ \hline \vee \\ \hline \end{array} \xrightarrow{UD} \begin{array}{|c|} \hline \wedge \\ \hline \vee \\ \hline \end{array}$$

which we denote by $T^{(1,2)}$ and S respectively. These three paths give rise to the elements pictured in Figure 23.



FIGURE 23. The diagrams c_{T^\emptyset} , $c_{T^{(1,2)}}$, and c_S . The first two elements are primitive central idempotents.

The modules $c_{T^\emptyset} \mathcal{H}_{P \setminus W}$ and $c_{T^{(1,2)}} \mathcal{H}_{P \setminus W}$ are projective indecomposable. These modules have bases $\{c_{T^\emptyset T^\emptyset}, c_{T^\emptyset S}\}$ and $\{c_{T^{(1,2)} T^{(1,2)}}, c_{T^{(1,2)} T^\emptyset}, c_{T^{(1,2)} S}\}$ respectively. We note that no forks appear in the basis of either module because the top and bottom each have at most one pink strand and hence can be simplified using the fork-spot relation of (S1). There are no barbells because these can be moved leftwards using (S2) and then annihilated by (S3). We have that $\mathcal{H}_{P \setminus W}$ decomposes as a direct sum of these two projective indecomposable modules.

The grading structure for the projective modules coincides with their submodule structure: to see this note that the algebra is non-negatively graded and that each homogeneous component of $c_{\tau\emptyset}\mathcal{H}_{P\setminus W}$ and $c_{\tau(1,2)}\mathcal{H}_{P\setminus W}$ is 1-dimensional. The action of the idempotents is obvious and the action of the other (non-zero) generator is encoded in Figures 24 and 25. The two simple modules are the 1-dimensional spaces spanned by the idempotents; these spaces are annihilated by the spot generators.

Injective homomorphisms between projective modules respect the Bruhat order, in particular there exists a unique

$$\Psi_{\emptyset\rightarrow(1,2)} \in \text{Hom}_{\mathcal{H}_{P\setminus W}}(c_{\tau\emptyset}\mathcal{H}_{P\setminus W}, c_{\tau(1,2)}\mathcal{H}_{P\setminus W})$$

given by left multiplication by the spot generator (and therefore this homomorphism has graded dimension q^1). We can define the standard or cell module $P(\lambda) \rightarrow \Delta(\lambda)$ to be the co-kernel of the injective homomorphisms from all other projective modules into $P(\lambda)$. Thus

$$\Delta(\emptyset) \cong P(\emptyset) \quad \Delta((1,2)) \cong P((1,2))/\text{Im}(\Psi_{\emptyset\rightarrow(1,2)}).$$

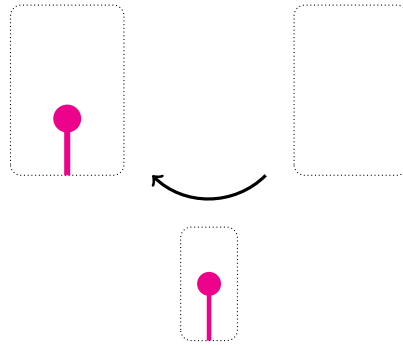


FIGURE 24. The submodule structure of $c_{\tau\emptyset}\mathcal{H}_{P\setminus W}$ and the action of $\mathcal{H}_{P\setminus W}$.

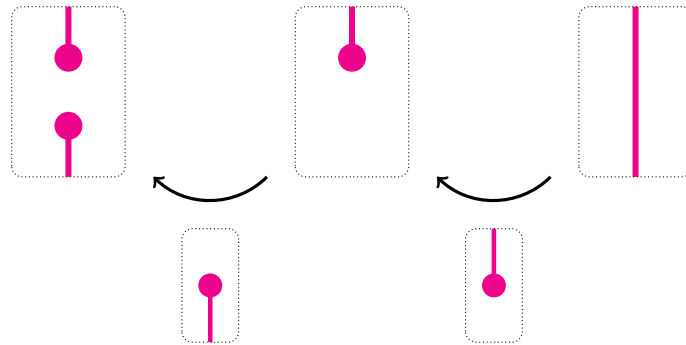


FIGURE 25. The submodule structure of $c_{\tau(1,2)}\mathcal{H}_{P\setminus W}$ and the action of $\mathcal{H}_{P\setminus W}$.

We have the two-colour relations left to consider. We suppose that $\sigma, \tau \in W$ are two non-commuting Coxeter reflections and $\rho, \tau \in W$ are two commuting Coxeter reflections. We have the two-colour barbell relation which allows us to move a barbell through a strand at the expense of two error terms, as follows:

$$\begin{array}{c} \text{circle} \\ \text{vertical pink line} \\ \text{blue barbell} \end{array} = \begin{array}{c} \text{circle} \\ \text{blue barbell} \\ \text{vertical pink line} \end{array} - \begin{array}{c} \text{circle} \\ \text{vertical pink line} \\ \text{pink barbell} \end{array} + \begin{array}{c} \text{circle} \\ \text{pink barbell} \\ \text{vertical pink line} \end{array} \tag{S4}$$

and the Temperley–Lieb relations

$$\begin{array}{|c|} \hline \text{Three vertical lines (two pink, one blue)} \\ \hline \end{array} = (-1) \begin{array}{|c|} \hline \text{A pink line crossing over a blue line} \\ \hline \end{array} \quad \begin{array}{|c|} \hline \text{Two vertical lines (one green, one blue)} \\ \hline \end{array} = \begin{array}{|c|} \hline \text{A green line crossing over a blue line} \\ \hline \end{array}. \quad (\text{S5})$$

We further have the parabolic-annihilation relation

$$\begin{array}{|c|} \hline \text{A single blue vertical line} \\ \hline \end{array} \otimes 1_{\mathfrak{S}} = 0 \quad (\text{S6})$$

for $\tau \in P = \mathfrak{S}_k \times \mathfrak{S}_{n-k}$. The remaining relations are all commutativity relations

$$\begin{array}{|c|} \hline \text{A blue line crossing over a green line} \\ \hline \end{array} = \begin{array}{|c|} \hline \text{A blue line crossing under a green line} \\ \hline \end{array}, \quad \begin{array}{|c|} \hline \text{A blue line crossing over a green line} \\ \hline \end{array} = \begin{array}{|c|} \hline \text{A blue line crossing over a green line} \\ \hline \end{array}, \quad \begin{array}{|c|} \hline \text{A blue line crossing over a blue line} \\ \hline \end{array} = \begin{array}{|c|} \hline \text{A blue line crossing over a blue line} \\ \hline \end{array}. \quad (\text{S7})$$

Remark 2.4. *The Temperley–Lieb relations can be seen as a manifestation of the defining relations for Temperley–Lieb diagrams*

$$\begin{array}{|c|} \hline \text{A diagram with two pink lines and one blue line, each having a loop} \\ \hline \end{array} = \begin{array}{|c|} \hline \text{A diagram with two pink lines and one blue line, each having a loop} \\ \hline \end{array}, \quad \begin{array}{|c|} \hline \text{A diagram with two blue lines and one green line, each having a loop} \\ \hline \end{array} = \begin{array}{|c|} \hline \text{A diagram with two blue lines and one green line, each having a loop} \\ \hline \end{array}$$

2.3. Cellularity and the Kazhdan–Lusztig positivity conjecture. We have already seen, in our toy example of \mathfrak{S}_2 , that Hecke categories possess graded bases which can encode a great deal of representation theoretic information. The formalism for this is provided by the framework of *cellularity*. In this section we prove the cellularity of our diagrammatic Hecke categories for $\mathfrak{S}_k \times \mathfrak{S}_{n-k} \leq \mathfrak{S}_n$. The cellularity formalism allows us to define the p -Kazhdan–Lusztig polynomials and to explain Elias–Williamson’s proof of the Kazhdan–Lusztig positivity conjecture.

Theorem 2.5 (Elias–Williamson, Libedinsky, Libedinsky–Williamson). *We have that $\mathcal{H}_{P \setminus W}$ is a \mathbb{Z} -graded of finite rank over \mathbb{Z} . Moreover the following hold*

- (1) *Each $c_{\mathfrak{S}\mathfrak{T}}$ is homogeneous of degree $\deg(c_{\mathfrak{S}\mathfrak{T}}) = \deg(\mathfrak{S}) + \deg(\mathfrak{T})$, for $\lambda \in \Lambda_{n,k}$ and $\mathfrak{S}, \mathfrak{T} \in \text{Path}(\lambda)$.*
- (2) *The set $\{c_{\mathfrak{S}\mathfrak{T}} \mid \mathfrak{S}, \mathfrak{T} \in \text{Path}(\lambda), \lambda \in \Lambda_{n,k}\}$ is a \mathbb{Z} -basis of $\mathcal{H}_{P \setminus W}$.*
- (3) *If $\mathfrak{S}, \mathfrak{T} \in \text{Path}(\lambda)$, for some $\lambda \in \Lambda_{n,k}$, and $a \in \mathcal{H}_{P \setminus W}$ then there exist scalars $r_{\mathfrak{S}\mathfrak{U}}(a)$, which do not depend on \mathfrak{T} , such that*

$$ac_{\mathfrak{S}\mathfrak{T}} = \sum_{\mathfrak{U} \in \text{Path}(\lambda)} r_{\mathfrak{S}\mathfrak{U}}(a) c_{\mathfrak{U}\mathfrak{T}} \pmod{\mathcal{H}^{\triangleright \lambda}}, \quad (\text{2.1})$$

where $\mathcal{H}^{\triangleright \lambda}$ is the \mathbb{Z} -submodule of $\mathcal{H}_{P \setminus W}$ spanned by $\{c_{\mathfrak{Q}\mathfrak{R}}^{\mu} \mid \mu \triangleright \lambda \text{ and } \mathfrak{Q}, \mathfrak{R} \in \text{Path}(\mu)\}$.

- (4) *The \mathbb{Z} -linear map $*$: $\mathcal{H}_{P \setminus W} \rightarrow \mathcal{H}_{P \setminus W}$ determined by $(c_{\mathfrak{S}\mathfrak{T}})^* = c_{\mathfrak{T}\mathfrak{S}}$, for all $\lambda \in \Lambda_{n,k}$ and all $\mathfrak{S}, \mathfrak{T} \in \text{Path}(\lambda)$, is an anti-isomorphism of $\mathcal{H}_{P \setminus W}$.*

In other words, $\mathcal{H}_{P \setminus W}$ is cellular, in the sense of Graham–Lehrer.

Before embarking on the proof, we first explore some of the consequences of this theorem. Given $\lambda \in \Lambda_{n,k}$, the graded cell module $\Delta(\lambda)$ is the graded left $\mathcal{H}_{P \setminus W}$ -module with basis $\{c_S \mid S \in \text{Path}(\lambda)\}$. The action of $\mathcal{H}_{P \setminus W}$ on $\Delta(\lambda)$ is given by

$$ac_S = \sum_{U \in \text{Path}(\lambda)} r_{SU}(a) c_U,$$

where the scalars $r_{SU}(a)$ are the scalars appearing in equation (2.1). Suppose that $\lambda \in \Lambda_{n,k}$. There is a bilinear form $\langle \cdot, \cdot \rangle_\lambda$ on $\Delta(\lambda)$ which is determined by

$$c_U c_T \equiv \langle c_S, c_T \rangle_\lambda c_{UV} \pmod{\mathcal{H}^{\triangleright \lambda}},$$

for any $S, T, U, V \in \text{Path}(\lambda)$. For every $\lambda \in \Lambda_{n,k}$, we let $\langle \cdot, \cdot \rangle_\lambda$ denote the bilinear form on $\Delta(\lambda)$ and let $\text{rad} \langle \cdot, \cdot \rangle_\lambda$ denote the radical of this bilinear form. We set $L(\lambda) = \Delta(\lambda) / \text{rad} \langle \cdot, \cdot \rangle_\lambda$. Each module $L(\lambda)$ is graded and simple, and in fact every irreducible $\mathcal{H}_{P \setminus W}$ -module is of this form, up to grading shift. We remark that the above specialises to the construction in Example 2.3 in that case.

Definition 2.6. We define the (anti-spherical) p -Kazhdan–Lusztig polynomials to be the

$${}^p n_{\lambda\mu}(q) = \sum_{k \in \mathbb{Z}} [\Delta(\lambda) : L(\mu)\langle k \rangle] q^k.$$

The composition series of standard modules for $\mathcal{H}_{P \setminus W}$ give a manifestly non-negative structural interpretation of these polynomials. As the name would suggest, the p -Kazhdan–Lusztig polynomials specialise to be the classical Kazhdan–Lusztig polynomials when $p = \infty$ as we will see in the following theorem. This theorem was first proven in the non-parabolic setting of \mathcal{H}_W by Elias–Williamson in [?]. This theorem was later generalised to the full generality of the anti-spherical setting $\mathcal{H}_{P \setminus W}$ by Libedinsky–Williamson in [LW].

Theorem 2.7 ([LW, Theorem 8.2 and Corollary 8.3]). *Over the complex field, we have that*

$$b_{\lambda\mu}(q) = \dim(1_{T^\mu} L(\lambda)\langle k \rangle) q^k \quad n_{\lambda\mu}(q) = \sum_{k \in \mathbb{Z}} [\Delta(\lambda) : L(\mu)\langle k \rangle] q^k.$$

In particular, the p -Kazhdan–Lusztig polynomials coincide with the classical definition of Kazhdan–Lusztig polynomials over a field of infinite characteristic.

Obviously Elias–Williamson and Libedinsky–Williamson work in the full generality of arbitrary (anti-spherical) Hecke categories, they do not limit themselves to our example of $\mathfrak{S}_k \times \mathfrak{S}_{n-k} \leq \mathfrak{S}_n$. The presentations of these categories are harder to get to grips with, but our example encapsulates a surprising amount of the work and serves as a springboard to the general case. Elias–Williamson deduced the following corollary:

Corollary 2.8 (The Kazhdan–Lusztig positivity conjecture). *For W an arbitrary Coxeter system, the coefficients appearing in the (p -)Kazhdan–Lusztig polynomials are non-negative.*

Example 2.9. *In Example 2.3 we saw that these polynomials are characteristic-free and are given by the matrix*

$$\begin{pmatrix} 1 & 0 \\ q & 1 \end{pmatrix}.$$

2.4. Submodule structures. Our Temperley–Lieb-style combinatorics allows us to explicitly calculate a great deal of information about submodule structures. In particular we can compute complete socle and radical filtrations, as follows:

Theorem 2.10 (B.–De Visscher–Hazi–Norton). *The socle, radical, and grading structures on $\mathcal{H}_{P \setminus W}$ -modules all coincide, for $P = \mathfrak{S}_k \times \mathfrak{S}_{n-k} \leq \mathfrak{S}_n = W$.*

Proof. This follows immediately from the fact that the subspace of degree zero elements $\mathcal{H}_{P \setminus W}$ is spanned by idempotents (which in turn follows from Theorem 1.22). \square

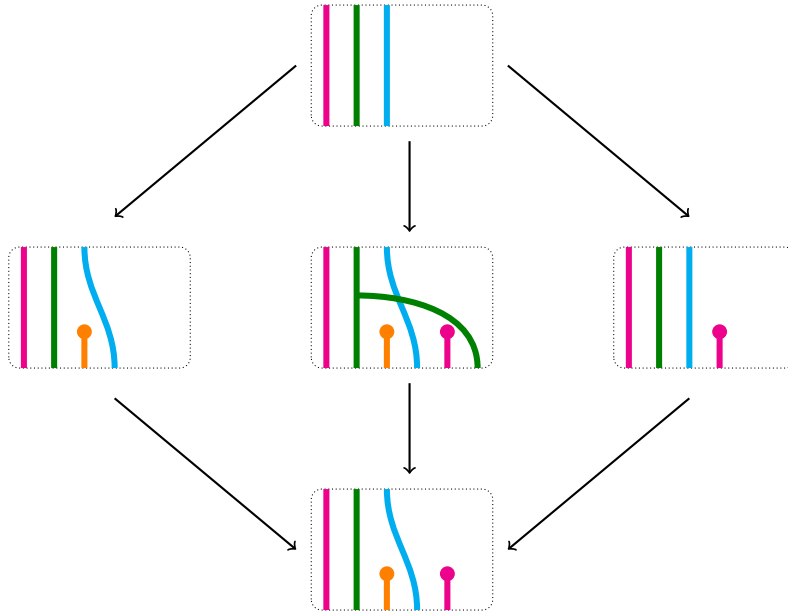


FIGURE 26. The $\mathcal{H}_{P \setminus W}$ -submodule structure of the 5-dimensional module $\Delta(s_2 s_3 s_1)$ for $P = \mathfrak{S}_2 \times \mathfrak{S}_3 \leq \mathfrak{S}_5 = W$.

Exercise 2.11. Using your answer to exercise 1.21 or otherwise, compute the full $\mathcal{H}_{P \setminus W}$ -submodule structure of the module $\Delta(\emptyset)$ for $P = \mathfrak{S}_2 \times \mathfrak{S}_3 \leq \mathfrak{S}_5 = W$.

2.5. Proof of cellularity in the case of $\mathfrak{S}_k \times \mathfrak{S}_{n-k} \leq \mathfrak{S}_n$. We remark that points (1) and (4) of Theorem 2.5 follow immediately from the definitions. Points (2) and (3) simply state that there is a chain of idempotent 2-sided ideals (generated by the idempotents 1_{τ^μ} corresponding to a preferred choice of reduced path for each $\mu \in \Lambda_{n,k}$) and that these ideals possess bases indexed by the paths in Bruhat graph.

Proof of Theorem 2.5. We first observe that any barbells within D can be moved to the left using S3 and S4 and annihilated using S4. Next we observe that we can take horizontal slices of D and (by isotopy if necessary) to obtain an idempotent for some configuration of boxes λ . We claim that we can apply rules to rewrite $1_\lambda = 1_{\sigma_1} \otimes \cdots \otimes 1_{\sigma_k}$ so that it factors through a partition. To see this, we note that if $\sigma_k = (r, c)$ does not correspond to an addable box, then either $(r, c - 1), (r - 1, c) \notin \lambda$ or both do not belong to λ . These can be pictured as

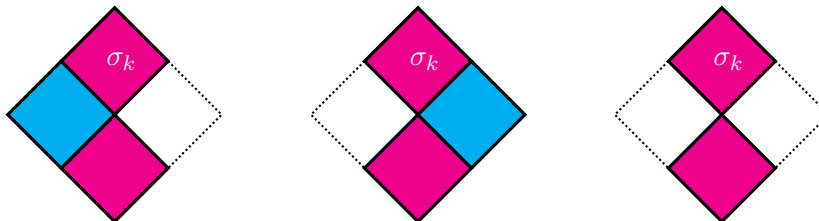


FIGURE 27. The cases where $(r, c - 1) \notin \lambda, (r - 1, c) \notin \lambda$ or both do not belong to λ , respectively. The first two can be simplified using S5 the latter with equation (2.2). Both can be thought of as “collapsing the tower” under gravity to obtain a single pink box (these also correspond to Temperley–Lieb relations).

In the former case (where only one does not belong to λ) we can apply the leftmost relation in S5 to simplify our diagram. In the latter case (where neither belongs) we can apply the

one-colour relations to rewrite

$$\text{Diagram} = \text{Diagram}_1 + \text{Diagram}_2 - \text{Diagram}_3 \quad (2.2)$$

and we observe that all of the resulting diagrams factor through words of shorter length. Thus we can cinch any diagram $D \in \mathcal{H}_{P \setminus W}$ so that it factors through an idempotent labelled by a reduced word as follows: $D = 1_{\mathbb{T}^\mu} a 1_{\mathbb{T}^\lambda} b 1_{\mathbb{T}^\nu} + \mathcal{H}^{< \lambda}$ for $\lambda \leq \mu, \nu$ (here $\mathcal{H}^{< \lambda}$ is the 2-sided ideal generated by idempotents strictly less than λ in the Bruhat ordering). By induction on the order \leq , it suffices to show that the subquotient

$$\{1_{\mathbb{T}^\mu} a 1_{\mathbb{T}^\lambda} b 1_{\mathbb{T}^\nu} + \mathcal{H}^{< \lambda} \mid a, b \in \mathcal{H}_{P \setminus W}\}$$

is equal to the span of the (unique) element $c_{\mathbb{S}\mathbb{T}}$ for $\mathbb{S} \in \text{SStd}(\lambda, \mathbb{T}^\mu)$, $\mathbb{T} \in \text{SStd}(\lambda, \mathbb{T}^\nu)$ if it exists, and is 0-dimensional otherwise. We do this for each side in turn. We can construct a spanning set for

$$\{1_{\mathbb{T}^\lambda} b 1_{\mathbb{T}^\nu} + \mathcal{H}^{< \lambda} \mid a, b \in \mathcal{H}_{P \setminus W}\}$$

by induction on the southern colour sequence \mathbb{T}^μ . At the k th step in \mathbb{T}^μ we let $\lambda(k)$ denote the northern colour sequence. We suppose that σ is the $(k+1)$ th colour in \mathbb{T}^μ . We have that $\sigma \in \text{Rem}(\lambda(k))$, $\sigma \in \text{Add}(\lambda(k))$, or neither of the above.

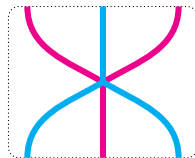
- If $\sigma \in \text{Rem}(\lambda(k))$ then we can either apply a σ -fork, a σ -strand, or a σ -spot. In the latter case, this is an element of the required form and so we are done. In the former two cases, we can rewrite the diagram using equation (2.2) to obtain a sum over three terms, all of which factor through words strictly less than λ in the Bruhat order, as required.
- If $\sigma \in \text{Add}(\lambda(k))$, then we can either apply a σ -strand, or a σ -spot. Either of which is an element of the required form.
- Finally if $\sigma \notin \text{Rem}(\lambda(k))$, or $\text{Add}(\lambda(k))$, then we are in one of the three cases depicted in Figure 27. We can rewrite the diagram in terms of elements strictly less than λ in the Bruhat ordering using S5 for the former two cases and equation (2.2) for the final case.

The result follows. \square

2.6. The general framework. Hecke categories are richer than their underlying Coxeter groups. When considering the general case (beyond the Temperley–Lieb like case of $\mathfrak{S}_k \times \mathfrak{S}_{n-k} \leq \mathfrak{S}_n$) we find that the “braid relations” of the Coxeter group are upgraded to “braid generators” of the Hecke category. In type A , these are lifts of the classical braid relations

$$\sigma\tau\sigma = \tau\sigma\tau$$

for σ and τ adjacent in the Coxeter graph. We lift this as follows: draw the colour sequence for each side of a Soergel diagram, then draw the naive diagram connecting the top and bottom colour sequences to obtain a new generator:



This diagram can be seen as the path-morphism between two distinct paths which terminate at the same point, for an example see Figure 28.

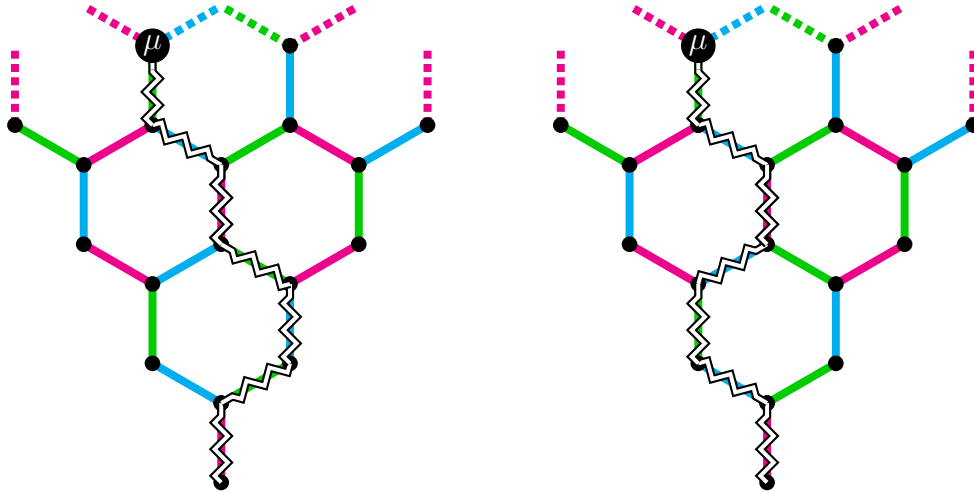


FIGURE 28. Two paths which differ by the application of a braid generator

Exercise 2.12. Draw the path-morphism between the paths in Figure 28.

We then have to consider lifts of “relations between relations” that is “what happens when we multiply by a braid generator”. The first of which is the Jones–Wenzl relations in type A . These replace the Temperley–Lieb relations (for $\mathfrak{S}_k \times \mathfrak{S}_{n-k} \leq \mathfrak{S}_n$) and are as follows,

$$\begin{array}{c} \circlearrowleft \\ \text{Diagram 1} \end{array} = \begin{array}{c} \circlearrowleft \\ \text{Diagram 2} \end{array} + \begin{array}{c} \circlearrowleft \\ \text{Diagram 3} \end{array} \tag{S6'}$$

Exercise 2.13. Verify that the local relation (S6) follows from the local relation (S6') together with the local relation $\text{braid}_{\tau\sigma\tau}^{\sigma\tau\sigma} = 0$. It is proven in [] that the parabolic annihilation relation for $\mathfrak{S}_k \times \mathfrak{S}_{n-k} \leq \mathfrak{S}_n$ implies that the local relation $\text{braid}_{\tau\sigma\tau}^{\sigma\tau\sigma} = 0$; this explains the “Temperley–Lieb-like” behaviour we have seen thus far.

We now picture the two-colour relations for non-commuting reflections $s_\sigma, s_\tau \in \widehat{\mathfrak{S}}_{hl}$. We have

$$\begin{array}{c} \circlearrowleft \\ \text{Diagram 1} \end{array} = \begin{array}{c} \circlearrowleft \\ \text{Diagram 2} \end{array} \quad \begin{array}{c} \square \\ \text{Diagram 3} \end{array} = \begin{array}{c} \square \\ \text{Diagram 4} \end{array} \tag{S9}$$

In order to picture the three-colour commuting relations we require a fourth Coxeter reflection $s_\delta \in \widehat{\mathfrak{S}}_{hl}$ which commutes with all other Coxeter reflections (such that $s_\delta s_\sigma = s_\sigma s_\delta$, $s_\delta s_\tau = s_\tau s_\delta$, $s_\delta s_\rho = s_\rho s_\delta$) and we have the following,

$$\begin{array}{c} \circlearrowleft \\ \text{Diagram 1} \end{array} = \begin{array}{c} \circlearrowleft \\ \text{Diagram 2} \end{array} \quad \begin{array}{c} \circlearrowleft \\ \text{Diagram 3} \end{array} = \begin{array}{c} \circlearrowleft \\ \text{Diagram 4} \end{array} \tag{S10}$$

Finally, we require the KZ relation for which we make the additional assumption on ρ that it does not commute with σ . This relation is as follows,

(S11)

Exercise 2.14. *The Bruhat graph of \mathfrak{S}_4 can be drawn as a 3-coloured permutahedron. The square faces correspond to commuting pairs of reflections and the hexagonal faces correspond to the non-commuting pairs of reflections. Recast the KZ relation in terms of this picture.*

3. p -DEPENDENT BEHAVIOUR IN HECKE CATEGORIES

The study of p -Kazhdan–Lusztig polynomials, ${}^p n_{x,y}$, can be roughly organised along two axes: one of these axes is the rank of the Weyl group W in question (roughly speaking, this corresponds to the number of colours in a Soergel diagram) and the other axis is the prime-power-depth of the labelling cosets $x, y \in W$ (roughly speaking, this corresponds to the number of strands in a Soergel diagram). Our understanding of these polynomials currently clings along these axes. For rank equal to 1, these polynomials were calculated by James some thirty years ago. For the prime-power-depth somewhere between 1 and 2 (but no-one quite knows where) these polynomials coincide with the classical Kazhdan–Lusztig polynomials, which are increasingly well-understood.

3.1. Lusztig’s, Andersen’s, and James’ conjectures. Lusztig’s conjecture stated that certain (dual) p -Kazhdan–Lusztig polynomials for $\mathfrak{S}_h \leq \widehat{\mathfrak{S}}_h$ were independent of the prime $p > h$. In order to obtain an appreciation of this conjecture in its historical setting, we will now introduce some of the basics of the representation theory of general linear group of $(h \times h)$ -invertible matrices, $\mathrm{GL}_h(\mathbb{k})$, and the symmetric group of n letters. Over the complex numbers the module categories of these groups are well-understood and equivalent, through the following theorem:

Theorem 3.1 (Schur 1901). *The n -fold tensor space $(\mathbb{C}^h)^{\otimes n}$ carries the structure of a $(\mathrm{GL}_h, \mathbb{C}\mathfrak{S}_n)$ -bimodule and decomposes as a direct sum of simple modules as follows*

$$(\mathbb{C}^h(\mathbb{C}))^{\otimes n} = \bigoplus_{\lambda \in \mathcal{P}_h(n)} V(\lambda) \otimes S(\lambda)$$

where $\mathcal{P}_h(n) = \{\lambda_1 \geq \lambda_2 \geq \dots \geq \lambda_h \geq 0 \mid \lambda_1 + \dots + \lambda_h = n\}$. We have that

$$\mathfrak{S}_n \rightarrow \mathrm{End}_{\mathrm{GL}_h(\mathbb{C})}((\mathbb{C}^h)^{\otimes n}) \quad \mathrm{GL}_h(\mathbb{C}) \rightarrow \mathrm{End}_{\mathfrak{S}_n}((\mathbb{C}^h)^{\otimes n}). \quad (3.1)$$

Lusztig’s and James’ conjectures were concerned with the representation theories of these groups over fields of finite characteristic. The endomorphism algebras in 3.2 are cellular algebras and so we can study them by reduction modulo p , in other words by understanding the composition factors of the Specht modules.

We embed $\mathcal{P}_h(n) \hookrightarrow \mathbb{R}\{\varepsilon_1, \varepsilon_2, \dots, \varepsilon_h\}$ and equip this space with the action of the affine Weyl group $\widehat{\mathfrak{S}}_h$. An example is depicted in Figure 29. The reflections partition the space into p -alcoves, in the case of Figure 29 these are triangles with edges of width p . One can also p -dilate this viewpoint and consider the p^2 -alcoves, in the case of Figure 29 these are triangles with edges of width p^2 . We refer to the p^i -alcove containing empty partition as the fundamental p^i -alcove.

Theorem 3.2 (Green–Lusztig). *The n -fold tensor space $(\mathbb{k}^h)^{\otimes n}$ carries the structure of a $(\mathrm{GL}_h(\mathbb{k}), \mathbb{k}\mathfrak{S}_n)$ -bimodule. We have that*

$$\mathfrak{S}_n \rightarrow \mathrm{End}_{\mathrm{GL}_h(\mathbb{C})}((\mathbb{k}^h)^{\otimes n}) \quad \mathrm{GL}_h(\mathbb{C}) \rightarrow \mathrm{End}_{\mathfrak{S}_n}((\mathbb{k}^h)^{\otimes n}). \quad (3.2)$$

The blocks of these endomorphism algebras are given by the orbits under the action of the affine Weyl group $\widehat{\mathfrak{S}}_h$.

We say that a partition $\lambda \in \mathcal{P}_h(n)$ is **regular** if it does not lie on any $\widehat{\mathfrak{S}}_h$ -hyperplane. We let $\mathcal{P}_h^{\mathrm{reg}}(n) \subseteq \mathcal{P}_h(n)$ denote the set of all regular partitions. The orbit of a regular partition can thus be identified with the Bruhat graph of $\mathfrak{S}_h \backslash \widehat{\mathfrak{S}}_h$. We say that a block of $\mathrm{End}_{\mathrm{GL}_h(\mathbb{k})}((\mathbb{k}^h)^{\otimes n})$ is regular if contains a regular partition (and therefore contains only regular partitions).

Theorem 3.3 (Riche–Williamson, Elias–Losev, B.–Cox–Hazi). *Let $p > h$. Any regular block of $\mathrm{End}_{\mathrm{GL}_h(\mathbb{k})}((\mathbb{k}^h)^{\otimes n})$ is Morita equivalent to the anti-spherical Hecke category $\mathcal{H}_{\mathfrak{S}_h \backslash \widehat{\mathfrak{S}}_h}$.*

Therefore the decomposition numbers of symmetric groups labelled by $\mathcal{P}_h^{\text{reg}}(n)$ are equal to p -Kazhdan–Lusztig polynomials.

Conjecture 3.4 (Lusztig’s and Andersen’s conjectures). *Let $\lambda, \mu \in \mathcal{P}_h(n)$ be points in the fundamental p^2 -alcove and $p > h$. Then the decomposition numbers of symmetric groups (respectively general linear groups) are given by the associated Kazhdan–Lusztig polynomials (respectively dual Kazhdan–Lusztig polynomials) of type $\mathfrak{S}_h \backslash \widehat{\mathfrak{S}}_h$.*

Thus Lusztig’s and Andersen’s conjectures state that certain (dual) p -Kazhdan–Lusztig polynomials are characteristic-free within the first p^2 -alcove. Williamson recently found counterexamples which disprove these conjectures unless p is, at the very least, exponentially larger than h .

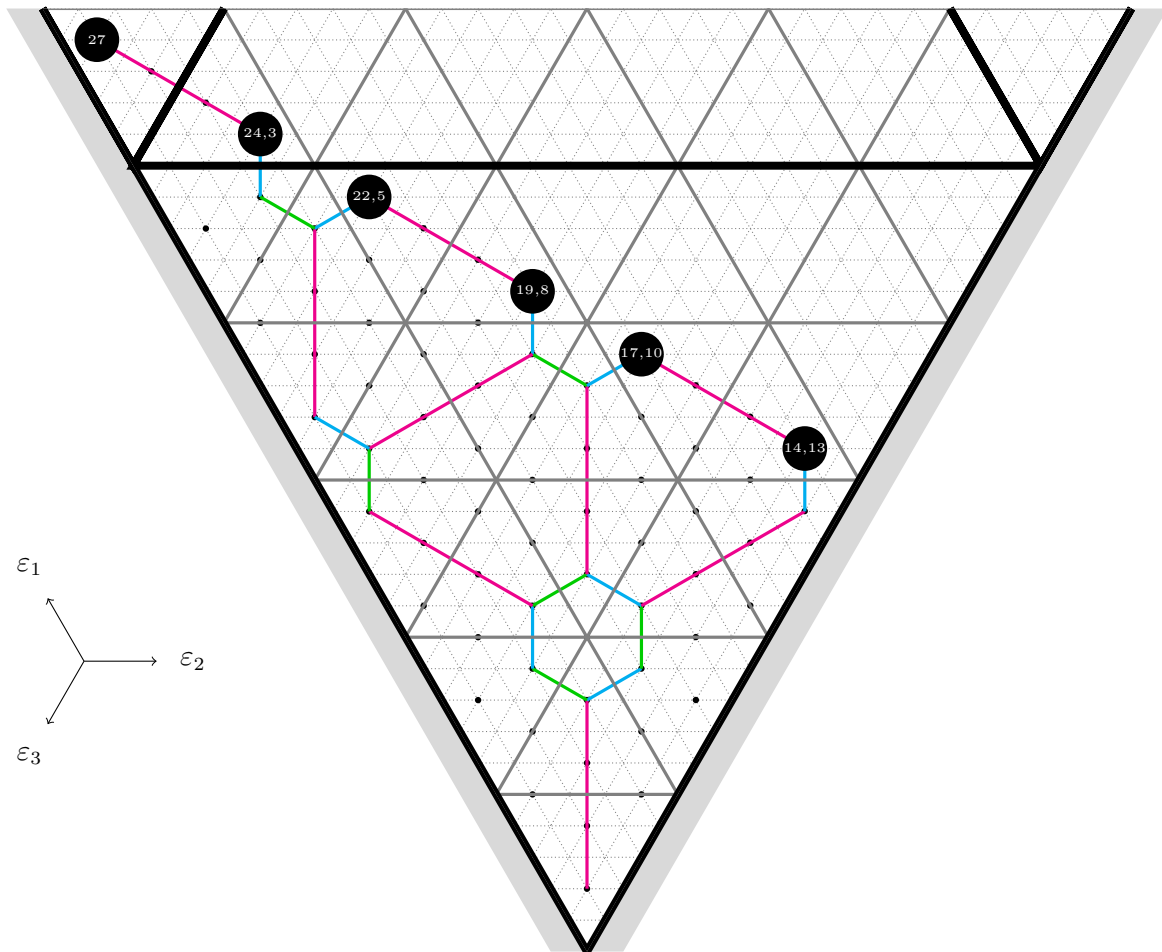


FIGURE 29. Embedding $\mathcal{P}_3(27) \hookrightarrow \mathbb{R}\{\varepsilon_1, \varepsilon_2, \varepsilon_3\}$. The action for $p = 5$ is depicted. We have labelled a few of the partitions for reference. We have highlighted the p^2 reflections as well.

3.2. Generational philosophy. Recent work of Elias, Hazi, Jensen, and Lusztig–Williamson, has developed a new approach to understanding all p -Kazhdan–Lusztig polynomials (at least for p incredibly large). The first explicit conjecture in this direction was made by Jensen–Lusztig–Williamson and it provides a combinatorial interpretation for ${}^p n_{\lambda, \mu}(q)$ for $\mathfrak{S}_3 \backslash \widehat{\mathfrak{S}}_3$ within the first p^3 -alcove in terms of a dynamical system of bouncing billiard balls.

3.3. The origins of p -dependent behaviour. We pose the following problem as a possible research question for a plucky and computationally-minded young researcher wanting to get into this field.

Research problem 3.5. *Classify the parabolic Coxeter systems (W, P) for which the anti-spherical p -Kazhdan–Lusztig are characteristic-free.*

We remark that certain maximal parabolic pairs (the Hermitian symmetric pairs (W, P)) of finite type do satisfy the property of being characteristic-free (this is proven in joint work with De Visscher Hazi and Norton). Our favourite example of a Hermitian symmetric pair is the pair $\mathfrak{S}_k \times \mathfrak{S}_{n-k} \leq \mathfrak{S}_n$ considered in depth in these lectures. It would be interesting if these were the only infinite families satisfying this property.

REFERENCES

[LW] N. Libedinsky and G. Williamson, *The anti-spherical category*, [arXiv:1702.00459](https://arxiv.org/abs/1702.00459).

Acknowledgements. *I have come to understand this material through my rewarding collaborations with Anton Cox, Maud De Visscher, and Amit Hazi.*

DEPARTMENT OF MATHEMATICS, UNIVERSITY OF YORK, HESLINGTON, YORK, YO10 5DD, UK
E-mail address: `Chris.Bowman-Scargill@york.ac.uk`